university of groningen

University Medical Center Groningen

University of Groningen

Decomposition of ethylamine through bimolecular reactions

Altarawneh, Mohammednoor; Almatarneh, Mansour H.; Marashdeh, Ali; Dlugogorski, Bogdan Z.

Published in:
Combustion and Flame

DOI:
10.1016/j.combustflame.2015.10.032

IMPORTANT NOTE: You are advised to consult the publisher's version (publisher's PDF) if you wish to cite from it. Please check the document version below.

Document Version
Publisher's PDF, also known as Version of record

Publication date:
2016

Link to publication in University of Groningen/UMCG research database

Citation for published version (APA):
Altarawneh, M., Almatarneh, M. H., Marashdeh, A., & Dlugogorski, B. Z. (2016). Decomposition of ethylamine through bimolecular reactions. *Combustion and Flame*, *163*, 532-539. https://doi.org/10.1016/j.combustflame.2015.10.032

Copyright
Other than for strictly personal use, it is not permitted to download or to forward/distribute the text or part of it without the consent of the author(s) and/or copyright holder(s), unless the work is under an open content license (like Creative Commons).

The publication may also be distributed here under the terms of Article 25fa of the Dutch Copyright Act, indicated by the “Taverne” license. More information can be found on the University of Groningen website: https://www.rug.nl/library/open-access/self-archiving-pure/taverne-amendment.

Take-down policy
If you believe that this document breaches copyright please contact us providing details, and we will remove access to the work immediately and investigate your claim.

Downloaded from the University of Groningen/UMCG research database (Pure): http://www.rug.nl/research/portal. For technical reasons the number of authors shown on this cover page is limited to 10 maximum.

Download date: 28-04-2023

Combustion and Flame 163 (2016) 532–539

Contents lists available at ScienceDirect

Combustion and Flame

journal homepage: www.elsevier.com/locate/combustflame

Decomposition of ethylamine through bimolecular reactions

Mohammednoor Altarawneh [a,*], Mansour H. Almatarneh [b], Ali Marashdeh [c,d], Bogdan Z. Dlugogorski [a]

[a] School of Engineering and Information Technology, Murdoch University, Perth, Australia
[b] Department of Chemistry, University of Jordan, Amman 11942, Jordan
[c] Department of Theoretical Chemistry, Zernike Institute for Advanced Materials, University of Groningen, Nijenborgh 4, 9747 AG Groningen, The Netherlands
[d] Department of Chemistry, Faculty of Science, Al-Balqa' Applied University, Salt, Jordan

ARTICLE INFO

Article history:
Received 31 May 2015
Revised 23 October 2015
Accepted 24 October 2015
Available online 24 November 2015

Keywords:
Ethylamine
Reaction rate constants
Nitrogen content in biomass
H abstraction reactions

ABSTRACT

Ethylamine (EA) often serves as a surrogate species to represent aliphatic amines that occur in biofuels. This contribution reports, for the first time, the thermochemical and kinetic parameters for bimolecular reactions of EA with three prominent radicals that form in the initial stages of biomass decomposition; namely, H, CH_3 and NH_2. Abstraction of a methylene H atom from the EA molecule largely dominates H loss from the two other sites (i.e., methyl and amine hydrogens) for the three considered radicals. We demonstrate that, differences in bond dissociation enthalpies of methylene C–H bonds among EA, ethanol and propane reflect their corresponding HOMO/LUMO energy gaps. At low and intermediate temperatures, the rate of H abstraction from the methylene site in EA exceeds the corresponding values for propane and ethanol. As the temperature rises, matching entropic factors induce comparable rate constants for the three molecules.

© 2015 The Combustion Institute. Published by Elsevier Inc. All rights reserved.

1. Introduction

Combustion chemistry of nitrogen content in fuels remains an active area of research [1-3]. In particular, interests in chemistry of nitrogen conversion in fuels are evident in two areas: (i) developing comprehensive mechanisms for emission of small nitrogenated pollutants (i.e. HCN, NH_3, HNO and HCNO) during combustion processes; and, (ii) re-evaluating the NO_X emission upon introduction of biofuels as additives or alternatives to conventional hydrocarbons fuels. In this regard, aliphatic amines constitute major nitrogen carriers in all types of biofuels [4]. Since ethylamine ($CH_3CH_2NH_2$ or EA for short) constitutes one of the simplest amine-containing species, it represents a surrogate species for aliphatic amines in recent combustion studies. For example, Lucassen et al. [5] carried out a comprehensive in-situ analysis of laminar premixed flames of EA for air-fuel equivalence ratios within a range of 0.8–1.3. These authors formulated a detailed reaction mechanism to account for profiles of product species and identified a large number of small nitrogenated species. Li et al. [6,7] investigated oxidation and pyrolysis of EA behind reflected shock waves, measuring time histories of NH_2 and constructing a mechanism to track the evolution of NH_2 emission histories. Rupture of the C–N bond in the EA molecule initiates its decomposition: [7].

$$CH_3CH_2NH_2 \rightarrow CH_3CH_2 + NH_2$$

In a recent theoretical study [8], we have mapped out pathways controlling the unimolecular decomposition of EA. Our estimated pressure-dependent reaction rate constant, calculated between 1.2 bar and 2.1 bar for the initiation channel, matches reasonably well the analogous experimental measurements of Li et al. [7]; i.e., within a factor of 2.4. A mechanistic sensitivity analysis [6] shows that, the initial C–N scission at low temperatures and C–C bond dissociation at higher temperatures (1330 K–1790 K) strongly influence the formation of NH_2 [6].

$$CH_3CH_2NH_2 \rightarrow CH_2NH_2 + CH_3$$

The mechanism of the oxidative decomposition of EA demonstrates that beside unimolecular pathways and H_2/O_2 reactions, bimolecular reactions of EA with radicals significantly affect the ignition delay times of EA and profiles of its product species [6]. H, CH_3 and NH_2 are among the most prominent radicals prevailing in the decomposition medium of EA. Currently, there are no experimental measurements or results of theoretical kinetic computations for reactions of these radicals with EA. In the oxidation mechanism of Lucassen et al. on morpholine [9] and EA [5] molecules, kinetic parameters of reactions of EA with these radicals originated from analogous reactions involving ethanol and propane. In this contribution, we aim to provide rate constants for reactions of EA with H, CH_3 and NH_2 radicals, and to assess the influence of –OH, $–CH_3$ and $–NH_2$ functional groups on kinetics of H abstractions from secondary sites in C_3 hydrocarbons.

* Corresponding authors:
E-mail addresses: m.Altarawneh@murdoch.edu.au (M. Altarawneh), m.almatarneh@ju.edu.jo (M.H. Almatarneh).

http://dx.doi.org/10.1016/j.combustflame.2015.10.032
0010-2180/© 2015 The Combustion Institute. Published by Elsevier Inc. All rights reserved.

2. Theoretical methodology

Gaussian09 suite [10] of programmes facilitates calculations of energies and structural optimisation at the composite chemistry model of CBS-QB3 [11]. The KiSThelP code [12] serves to estimate reaction rate constants according to the conventional transition state theory (TST). A one-dimensional Eckart barrier accounts for quantum-tunnelling contribution [13]. Corrections for quantum mechanical tunnelling based on an unsymmetrical Eckart potential energy barrier depend on the magnitude of the imaginary frequencies in transition states and hence on the theoretical methodology. To test the reliability of the B3LYP in deriving transmission tunnelling factors, Fig. S1 in the supplementary information (SI) portrays tunnelling factors for H abstraction reactions from the secondary site in the EA molecule by the three title radicals based on the B3LYP/6 – 311 + G(d,p) and the M062X/6-311+G(d,p) level of theories [14]. Estimated tunnelling factors through an Eckart barriers by the meta hybrid DFT method of M062X noticeably exceed analogous values by the B3LYP method in the low temperature window, i.e., at temperatures lower than 600 K. Above this temperature, tunnelling factors calculated by the two methods appear very similar, i.e., within factors of 1.03–1.16. Figure S1 shows minimal contribution from the tunnelling effects based on the two theoretical approaches, at elevated temperatures. Bearing in mind that the reactions investigated herein become practically important at intermediate and high temperatures, we elect to implement the B3LYP method (the optimisation step in the CBS-QB3 model) in accounting for the tunnelling effects.

Hydrogen abstraction reactions are often associated with minimal variational effects [15]. In order to provide a benchmark comparison between rate constants obtained by the TST versus the corresponding values computed from the variational transition state theory (VTST), we give in Table S1 in the SI document reaction rate coefficients calculated by TST and VTST for two selected hydrogen abstraction reactions. We calculate reaction rate coefficients from VTST by considering minimum energy points (MEPs) in the reaction coordinate range of –0.20–0.20 bohr. Tables S2 and S3 assemble the potential energies, moment of inertia and vibrational frequencies of the considered MEPs, whereas Fig. S3 shows their corresponding energy profiles. For the reaction EA + H → CH_3CHNH_2 + H_2, we found that, the ratio k_{TST}/k_{VTST} holds constant at 1.16 throughout the entire temperature range. For the reaction EA + H → CH_3CHNH_2 + H_2, values of k_{TST}/k_{VTST} decreases gradually with temperature, i.e., from 1.38 at 300 K to 1.10 at 1000 K. This indicates that deploying VTST in estimating reaction rate constants does not improve the calculated constants over those obtained by the conventional TST. However, it is worthwhile mentioning that, variational effects depend on the reaction under investigation. Certain reactions display significant variational effects while the influence is minimal for others [16,17].

While it seems straightforward to determine the symmetry numbers of reactions, the task becomes challenging in some cases, [18] i.e., for symmetric reactions, reactions with conformers, in the presence of chiral transition structures and for symmetric reactions. Herein, we take into consideration total reaction degeneracies in each case by multiplying a symmetry number of each reaction (i.e., symmetry number of separated reactants/symmetry number of the transition state) by the number of abstractable hydrogen atoms. We calculate barrier heights for H abstractions from similar hydrogen atoms to be comparable (i.e., within 0.1 kJ/mol) enabling to treat these transition structures as effectively identical. This leads to reaction degeneracies of 3, 2 and 2 for H abstraction by H atoms from primary, secondary and amine sites; respectively. Corresponding reaction degeneracies for H abstraction by CH_3 and NH_2 are 18, 12 and 12, and 6, 4 and 4, respectively.

In estimating the kinetic parameters, we treat all internal rotations in reactants and transition structures as hindered rotors. The KiSThelP code adopts the approach of McClurg et al. [19] in treating

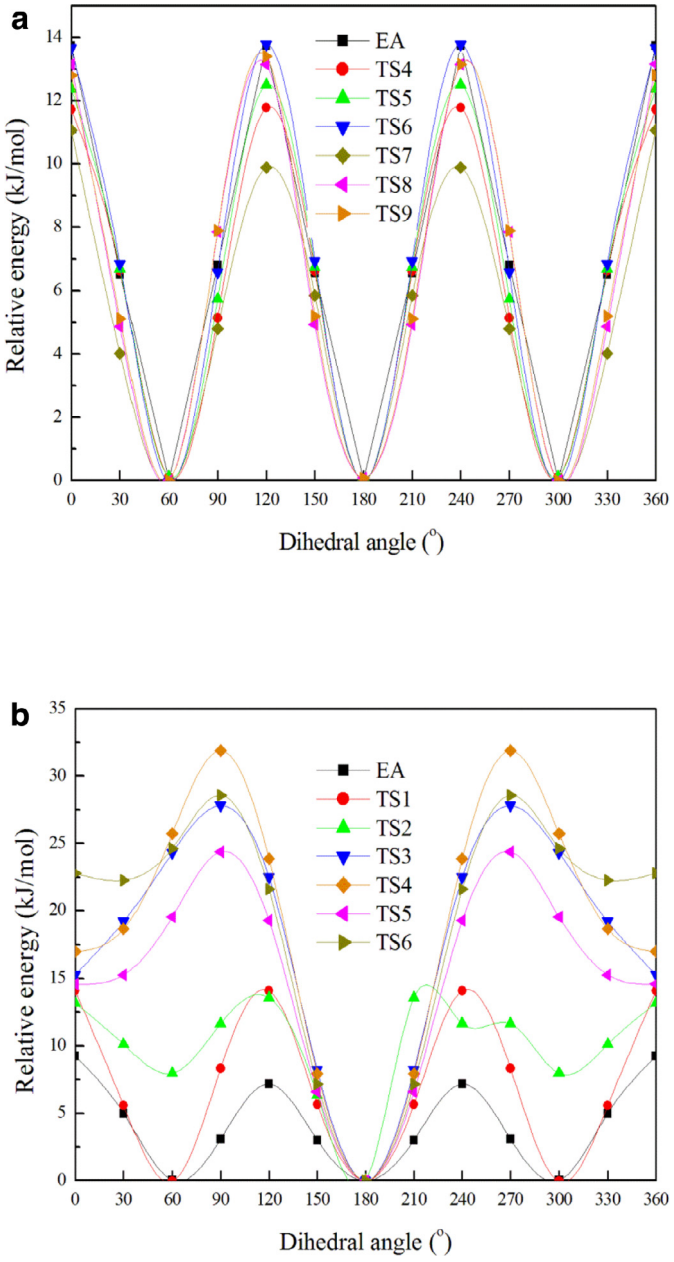

Fig. 1. Rotor potentials for the internal rotations of methyl (a) and amine (b) groups in the EA molecule and transition structures.

hindered rotors. This method interpolates between quantum-mechanical partition function at low temperature and the classical partition function at elevated temperatures. In this formalism, corrections to thermochemical values are based on three quantities, the overall rotational barrier of the internal rotors, their assigned vibrational frequencies and their symmetry numbers. The Supplementary Information (SI) document enlists barrier heights of the rotors (in the EA molecule and all transition structures) and their corresponding vibrational frequencies.

We calculate rotor potentials by performing partial optimisation around corresponding dihedral angles at an interval of 30° at the B3LYP/6–311+G(d,p) level of theory. To preserve the geometries of transition structures, atomic coordinates involved in breaking and forming bonds remained frozen while allowing the rest of the moiety to relax. Figure 1 portrays the 3-fold rotor potentials of methyl and amine groups in the EA molecule and all transition structures. For a clearer representation of the rotors potentials, we set the dihedral

Table 1
Calculated reaction enthalpies (ΔH), activation enthalpies ($\Delta H^{\#}$) at 298.15 K and reaction rate parameters (A and E_a) for reactions of EA molecule with H, CH_3, and NH_2 radicals. Arrhenius parameters are fitted between 300.0 and 2000.0 K. Values of ΔH are in kJ, $\Delta H^{\#}$ and E_a in kJ/mol, whereas A in cm^3/(molecule s).

Reaction	ΔH	$\Delta H^{\#}$	A	E_a
$EA + H \rightarrow CH_2CH_2NH_2 + H_2$	−18.4	37.5	2.66×10^{-11}	34.2
$EA + H \rightarrow CH_3CHNH_2 + H_2$	−60.2	14.5	1.92×10^{-11}	15.0
$EA + H \rightarrow CH_3CH_2NH + H_2$	−27.4	31.5	9.09×10^{-12}	28.9
$EA + CH_3 \rightarrow CH_2CH_2NH_2 + CH_4$	−27.9	49.2	9.97×10^{-12}	52.8
$EA + CH_3 \rightarrow CH_3CHNH_2 + CH_4$	−69.7	28.3	2.05×10^{-11}	33.1
$EA + CH_3 \rightarrow CH_3CH_2NH + CH_4$	−36.9	37.4	3.71×10^{-12}	39.5
$EA + NH_2 \rightarrow CH_2CH_2NH_2 + NH_3$	−18.6	34.9	1.53×10^{-11}	39.3
$EA + NH_2 \rightarrow CH_3CHNH_2 + NH_3$	−60.3	8.2	1.33×10^{-11}	19.8
$EA + NH_2 \rightarrow CH_3CH_2NH + NH_3$	−27.6	17.9	3.55×10^{-12}	24.8

angle for each rotor at 0º before carrying out the partial optimisations. Figure S3 depicts rotor potentials for the CH_3 and NH_2 abstracting radicals in two selected transition structures. Calculated barriers for the internal rotations of methyl and amine groups in the EA molecule amount to 13.9 kJ/mol and 9.8 kJ/mol, respectively. The former value accords with a corresponding experimental measurement of 15.5 kJ/mol [20]. The two minima in the $-NH_2$ curve signify *R-trans* and *R-gauche* conformers in the EA molecule. As Fig. 1 (a) shows, overall barriers of internal rotations of the methyl and amine groups in transition structures differ from the analogous values in the EA molecule. This signifies the importance of calculating internal rotations in transition structures rather than adapting their corresponding energy potentials from the parent EA molecule.

Among numerous methods estimating atomic charges, Hirshfeld [21] and Voronoi deformation density (VDD)[22] approaches provide the most accurate electronic partial charges [22]. Other methods, such as [22] Mulliken's charges, are very sensitive to the deployed basis set, while the Bader's scheme often yields unrealistic ionic character, even for covalent bonds. Thus, we calculate partial charges on EA, methanol, and propane molecules based on Hirshfeld and VDD schemes. We employ the ADF code [23] to estimate partial atomic charges. HOMO/LUMO related information (their involved fragments and energies) are generated automatically during structural optimisation.

3. Results and discussion

EA possess three distinct C–H bonds, methyl (or primary), methylene (or secondary) and N–H bonds. Computed bond dissociation enthalpies (BDH) at 298.15 K for primary C–H, secondary C–H and N–H bonds reach 422.4 kJ/mol, 380.6 kJ/mol and 413.4 kJ/mol, correspondingly. Our calculated BDH for methylene C–H bounds concurs very well with the corresponding experimental measurement of 377.0 ± 8.4 kJ/mol [24]. The significant difference in BDHs between the secondary C–H bonds and primary C–H/N–H bonds indicates that, decomposition of EA mainly passes through the methylidyne-like radical CH_3CHNH_2.

Table 1 enlists calculated standard reaction enthalpies (ΔH), activation enthalpies ($\Delta H^{\#}$), and fitted Arrhenius rate parameters for H abstractions from the EA molecule by the three title radicals. Calculated $\Delta H^{\#}$ values correlate with the BDHs. Figure 2 exhibits prominent geometrical features in transition structures for reactions in Table 1. Abstraction of H atoms from methylene sites incurs significantly lower $\Delta H^{\#}$ values if compared with H abstractions from the two other locations for the reaction of EA with the three radicals, see Table 1. For example, the $\Delta H^{\#}$ value for abstraction of methylene H by an H atom amounts to 14.7 kJ/mol, whereas corresponding values for abstraction from the methyl and amine sites equate to 37.5 kcal/mol and 31.6 kJ/mol, respectively. Inspection of calculated reaction rate constants reveals that, bimolecular reactions of H, CH_3 and NH_2 radicals largely lead to an H abstraction from the methylene site. Between 800 and 1600 K, branching ratios for abstraction of methylene H by H, CH_3 and NH_2 fall in the windows of 0.89–0.79, 0.91–0.81 and 0.85–0.69, respectively. Contributions to the H abstraction by the three title radicals from methyl and amine sites are very comparable throughout the considered temperature interval. Our present finding

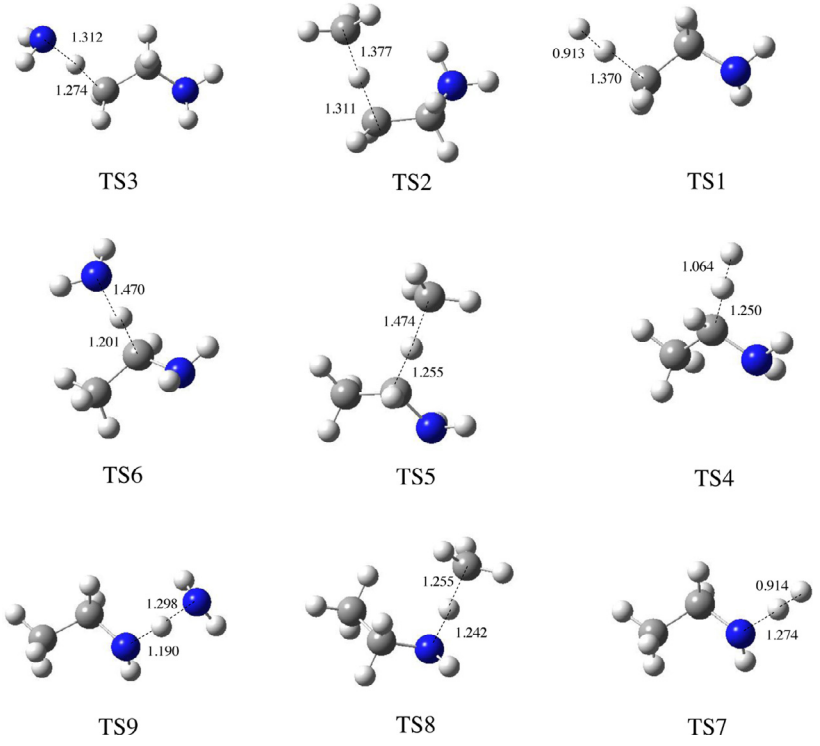

Fig. 2. Geometries of transition structures for H abstraction reactions from the EA molecule. Distances are in Å.

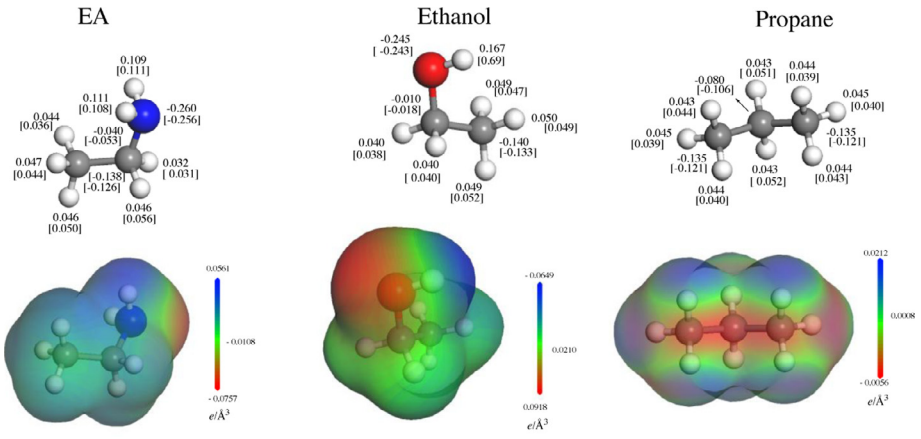

Fig. 3. Hirshfeld and VDD electronic charges (in e), and electronic densities (in $e/Å^3$) for EA, propane and ethanol. VDD electronic charges are given in brackets.

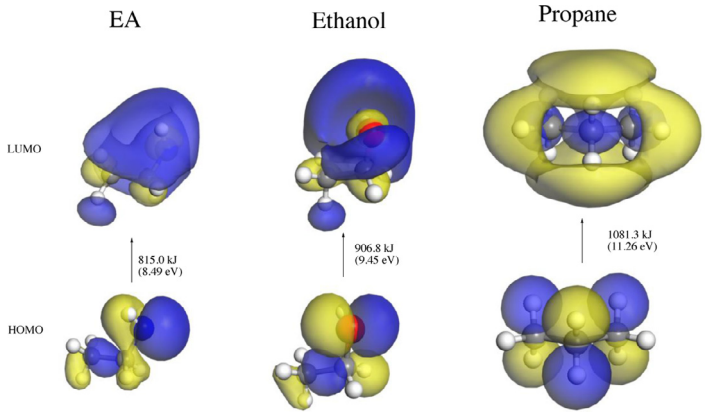

Fig. 4. HOMO and LUMO in EA, ethanol, and propane molecule and their associated energies.

of the dominance of H abstractions from the methylene site agrees with the recent experimental measurements for reactions of OH radicals with the EA molecule [25] and with the kinetic analysis of Lucassen et al. on oxidation of EA [5].

Available experimental values analogous to kinetic parameters reported in Table 1 are limited for the reaction of EA + CH_3 [26,27]. Figure 5 contrasts our calculated rate coefficients with analogous experimental values. Our estimated reaction rate constants for the reaction EA + CH_3 → CH_3CH_2NH + CH_4 at 400 K (2.57×10^{-17} cm^3/(molecule s)) remains in a good agreement with the corresponding experimental value of Brinton [26] (3.49×10^{-17} cm^3/(molecule s)). Between 383 and 453 K, and by utilising $2CH_3$ → C_2H_6 as a reference reaction, Gray and Jones [27] fitted reaction rate constants for H abstractions from the methylene and amine sites by CH_3 radicals to rate expressions of $k(T) = 2.49 \times 10^{-13}$ exp[−33 900/(R T)] cm^3/(molecule s) and $k(T) = 1.32 \times 10^{-14}$ exp[−27 100/(R T)] cm^3/(molecule s), respectively. At 400 K, our calculated rate constants overshoot analogous experimental values by almost one and two order of magnitudes for abstraction from the methylene and amine sites, correspondingly. Nonetheless, the reliability of the experimental measurements by Gray and Jones [27] can be questioned based on three focal points. First of all, activation energy for abstraction from the amine site in experimental rate expressions (i.e. 27.1 kJ/mol) falls below that of the methylene site (33.9 kJ/mol) in contrast to the trend of BDHs, i.e. 413.4 kJ/mol (amine site) versus 380.6 kJ/mol (methylene site). Secondly, the branching ratios based on the experimental measurements of Gray and Jones [27] seem to contradict the general consensus [5,25] that, abstraction from the methylene site largely predominates abstraction from the amine site. At 400 K, branching ratio for H abstraction from the amine site by a methyl group amounts to 0.29. Finally, the experimental value of reaction rate constant at 400 K for EA + CH_3 → CH_3CH_2NH + CH_4 of Gray and Jones [27] is lower by one order of magnitude when compared with the analogous value of Brinton [26].

Literature provides no experimental measurements or theoretical estimations for kinetic parameters reactions of the EA molecule with H and NH_2 radicals. However, various studies, performed under different operational conditions, report rate constants for reactions of the three title radicals with propane and ethanol. Reporting rate constants for reactions of H, CH_3 and NH_2 radicals with propane and ethanol serves two purposes; firstly, to set a benchmark of accuracy of our reported kinetic parameters for EA and, secondly, to gain insights into the effect of the neighbouring functional groups on rate constants for H abstractions from methylene carbons.

Table 2
Calculated reaction enthalpies (ΔH), activation enthalpies ($\Delta H^{\#}$) at 298.15 K and reaction rate parameters (A and E_a) for abstraction of methylene H atoms from propane and ethanol molecules by H, CH_3, and NH_2 radicals. Arrhenius parameters are fitted between 300.0 and 2000.0 K. Values of ΔH are in kJ, $\Delta H^{\#}$ and E_a in kJ/mol, whereas A in cm^3/(molecule s).

Reaction	ΔH	$\Delta H^{\#}$	A	E_a
$CH_3CH_2CH_3 + H \rightarrow CH_3CHCH_3 + H_2$	−26.8	26.8	3.86×10^{-11}	24.2
$CH_3CH_2CH_3 + CH_3 \rightarrow CH_3CHCH_3 + CH_4$	−27.0	45.6	2.41×10^{-12}	43.5
$CH_3CH_2CH_3 + NH_2 \rightarrow CH_3CHCH_3 + NH_3$	−36.4	26.8	5.67×10^{-13}	22.1
$CH_3CH_2OH + H \rightarrow CH_3CHOH + H_2$	−41.9	19.5	3.65×10^{-11}	18.2
$CH_3CH_2OH + CH_3 \rightarrow CH_3CHOH + CH_4$	−42.1	40.0	2.41×10^{-12}	36.5
$CH_3CH_2OH + NH_2 \rightarrow CH_3CHOH + NH_3$	−51.5	20.4	4.27×10^{-12}	19.5

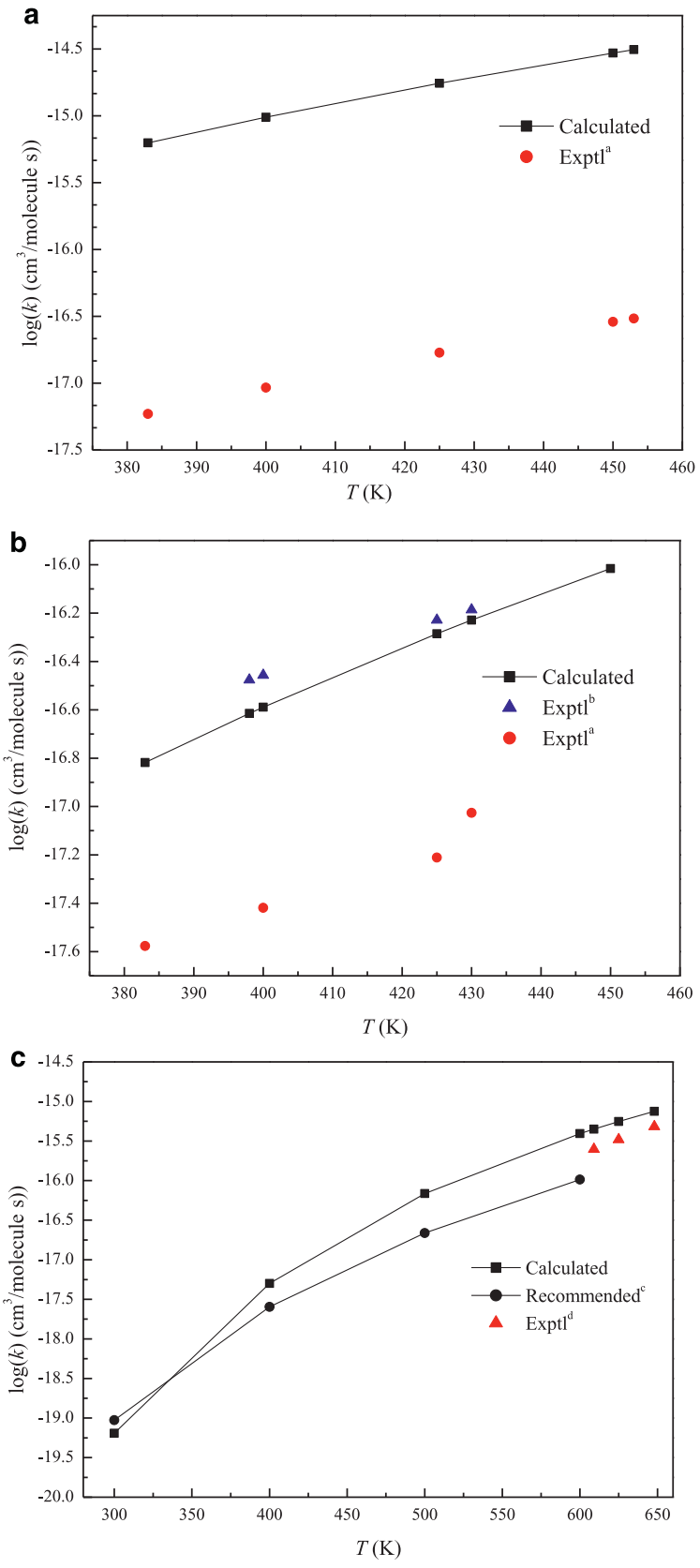

Fig. 5. Comparison between calculated and experimental values of reaction rate coefficients for H abstraction from primary (a), amine (b) and between calculated values for H abstraction from the secondary cite in propane with available literature data (c). [a]Ref 27, [b]Ref 26, [c]Ref 29, [d]Ref 28.

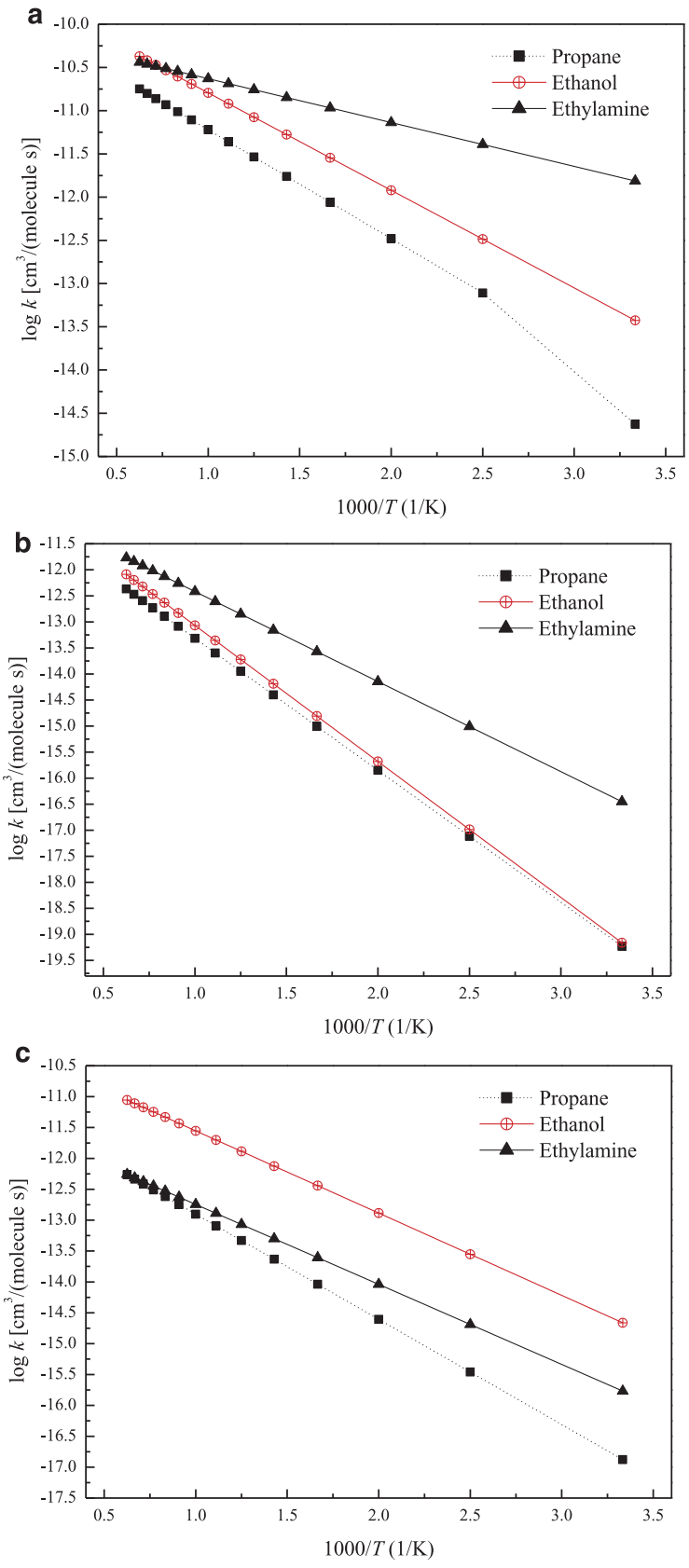

Fig. 6. Comparison among Arrhenius plots for abstraction of methylene hydrogen from propane, ethanol, and ethylamine by H (a), CH_3 (b) and NH_2 (c) radicals.

Methylene C–H bonds in ethanol and propane are weaker than other H–C/O bonds. Our computed BDHs for methyl H in ethanol and propane amount to 398.9 kJ/mol and 414.0 kJ/mol, correspondingly. These two values approach closely the recommended experimental measurements of 396.6 kJ/mol and 410.5 kJ/mol, respectively [24]. Table 2 provides ΔH, $\Delta H^{\#}$ and Arrhenius rate parameters for abstractions of methylene H from ethanol and propane by H, CH_3 and NH_2 radicals. BDHs for secondary C–H bonds in ethanol are slightly lower than the corresponding bonds in propane. Consequently, the calculated value of $\Delta H^{\#}$ for propane marginally exceeds that for ethanol.

Next, we turn our attention to comparing kinetic parameters in Table 2 with their analogous literature values with the aim of providing an accurate benchmark for the title reactions with the EA molecule. Our calculations of the rate parameters for abstraction of H by CH_3 radicals from ethanol and propane yield satisfactory agreement with experimental measurements available in literature. For example, Marshall et al. [28] obtained a rate constant $k(T) = 1.07 \times 10^{-11}$ exp[−21 800/(R T)] cm^3/(molecule s) for the reaction $C_3H_8 + H \rightarrow i\text{-}C_3H_7 + H_2$ over the temperature range 298–370 K. Our estimates of A (3.65×10^{-11} cm^3/(molecule s)) and E_a (24.2 kJ/mol) for this reaction coincide with the values of Marshall et al. Our estimated $k(T = 2000$ K) value for the reaction $CH_3CH_2CH3 + CH_3 \rightarrow CH_3CHCH_3 + CH_4$ (3.08×10^{-14} cm^3/(molecule s)) is in a very good agreement with the recommended value of Tsang [29] (1.13×10^{-14} cm^3/(molecule s)) and another theoretically-derived value of Hidaka et al. [30] (2.66×10^{-14} cm^3/(molecule s)). Finally, Fig. 5c contrasts our calculated rate coefficients for H abstraction from the secondary site in propane with analogous literature data [28,29] to report a satisfactory agreement.

Due to lower BDHs of methylene H bonds in EA (380.6 kJ/mol) in reference to corresponding bonds in propane (414.0 kJ/mol) and ethanol (398.9 kJ/mol), $\Delta H^{\#}$ for abstractions of secondary H from EA display lower values. Intuitively, this deviation in BDHs may arise from distinct charge distributions in the three molecules. Recently, we have thoroughly investigated the effect of electronic charge distribution on calculated reaction rate constants for dehydrohalogenation of ethyl halides [31]. In Fig. 3, we record estimated Hirshfeld and VDD partial charges (in e) and electronic densities (in e/Å^3) for EA, propane, and ethanol. Both schemes yield very similar atomic charges.

Calculated partial charges by the two methods confirm the nature of hydroxyl and amine groups as electron withdrawing groups by induction (–I). Noticeable difference in BDHs between methylene C–H bonds in EA and propane coincides with a more ionic character for methylene C–H bonds in propane in reference to corresponding bonds in the EA molecule, i.e. δ^+ (0.052 e) → δ^- (0.106 e) in propane versus δ^+ (0.031 e) → δ^- (0.053 e) in EA based on VDD charges. However, a lower bond polarisation for methylene C–H bonds in ethanol, i.e. δ^+ (0.038 e) → δ^- (0.018 e) in comparison with corresponding values in EA, does not enable drawing a conclusive statement with regard to the dependence of trends in BDHs values on their corresponding bond polarisation.

Energy gap between HOMO and LUMO (E^{L-H}) often serve as an indicator for relative stability of molecules; the larger the value of E^{L-H}, the greater the stability of molecule toward further chemical transformations, either via unimolecular or bimolecular reactions [32]. Figure 4 shows HOMO and LUMO for EA, ethanol, and propane molecules along with their associated E^{L-H} values. Clearly, estimated E^{L-H} values for EA (815.0 kJ), ethanol (906.8 kJ), and propane (1081.3 kJ) match analogous BDHs values for methylene C–H bonds in the three molecules; i.e., 373.3 kJ/mol, 392.4 kJ/mol and 407.0 kJ/mol, respectively.

Along the same line of enquiry, it has been reported that, electronegative oxygen atoms in ethers facilitate H abstraction by Br from its adjacent –CH_2- sites in comparison to neat hydrocarbon alkanes [33].In order to shed light onto this experimental observation, in view of the interplay between BDHs and E^{L-H} values, we calculate E^{L-H} for methoxyethane and the BDH for its methylene C–H as 892.7 kJ and 394.2 kJ/mol, correspondingly. Interestingly, ethanol and methoxyethane hold very similar values of E^{L-H} and the BDH for methylene C–H bonds. This infers a dependence of BDHs values for the weakest bonds in molecules on their E^{L-H} values. The decrease of E^{L-H} values in the series propane > ethanol > EA could be attributed to the fact that the HOMO goes from σ CH bonds to tight lone pair on O atom (ethanol) and to looser pair on the N atom (EA). It is worthwhile mentioning that, while the trends of E^{L-H} values correlate well with values of BDHs, E^{L-H} values could not explain in their own right the relative ordering of $\Delta H^{\#}$ values. The ordering of both $\Delta H^{\#}$ and BDHs might stem from the resonance ability in transition states and products. In this regard, the i-propyl radical offers no resonance stability whereas the strong electron-withdrawing group OH provides only limited resonance stability of the CH_3CHOH radical. More rigorous assessment of various types of bonds is needed to establish definite correlations between E^{L-H} and values of the BDHs.

To elucidate further a correlation between values of the BDH and $\Delta H^{\#}$, we show the Evans–Polanyi plots in Fig. S4. A clear linear relationship only appears for abstraction by H atoms. Evidently, the inclusion of only three points has not enabled detailed testing of the linearity correlation. Nonetheless, the three abstraction reactions in Fig. S3 hold very comparable slopes (i.e., 0.44–0.54). This in turn indicates that, the values of $\Delta H^{\#}$ strongly correlate with the estimates of BDH across the three abstraction radicals. Moreover, least-squares slopes are within the expected range of those of the Evans–Polanyi plots (0.0–1.0), and in accord with analogous values obtained for H abstraction from alkanes by RO_2 species, i.e., 0.60–0.65 [34].

Figure 6 compares Arrhenius plots for abstraction of secondary H by the three title radicals from EA, ethanol, and propane. In this figure, the energy term in the Arrhenius expression translates to a higher rate of H abstraction from the EA molecule by H and CH_3 radicals at temperatures as high as ~ 1000–1200 K. Beyond this temperature range, matching entropic factors (i.e. similar A factors) induce comparable rate constants for the three molecules as the temperature rises.

Available kinetic models for oxidative decomposition of EA[6] have adopted the corresponding bimolecular reactions of ethanol with H and CH_3 radicals. In the intermediate temperature range of 600–800 K (i.e., most relevant to formation of NO_X), our estimated rates of reactions EA/ethanol with the three title radicals are within factors of 3.8–2.1 (H), 17.4–7.4–(CH_3) and 14.7–15.2 (NH_2). Some of these ranges most likely falls within the expected accuracy margin of our estimated $E^{\#}$ and the adopted procedure of calculating the reaction rate constants (i.e., the TST/Eckart/hindered rotor treatment). Within the same temperature interval, the difference in estimated rate constants for EA + H/CH_3 and propane + H/CH_3 is rather more noticeable as Fig. 5 depicts.

4. Conclusions

Despite noticeable differences in BDHs and $\Delta H^{\#}$, calculated rate constants for abstraction of methylene H from the EA molecule by H/CH_3/NH_2 radicals deviate modestly from values for corresponding reactions involving propane and ethanol, especially at temperatures higher than 600 K. We have validated our estimated thermochemical and kinetic parameters against available experimental data in literature. Estimated Arrhenius parameters for reactions in Table 1 constitute the first kinetic account of rate constants for the bimolecular reactions of EA with the three title radicals. Reaction rate constants for H abstractions from the methylene sites in EA deviate considerably from corresponding values for propane at temperatures lower than 600 K, however, the discrepancy is rather modest between EA and ethanol at all temperatures. Having established the methylidyne-like radical CH_3CHNH_2 as the predominant product from the investigated bimolecular reactions, it would be insightful to map

out subsequent unimolecular decompositions steps of CH_3CHNH_2 toward the formation of chief experimental products, such as HCN, $H_3C–C{\equiv}N$ and $H_2C{=}NH$.

Acknowledgement

This study has been supported by grants of computing time from the National Computational Infrastructure (NCI) Australia, and the Pawsey Supercomputing Centre in Perth, as well as funds from the Australian Research Council (ARC). M. H. A. is grateful to the Atlantic Computational Excellence Network (ACEnet) for computer time. We thank reviewers for their useful and detailed comments that helped us to improve th manuscript.

Supplementary materials

Supplementary material associated with this article can be found, in the online version, at doi:10.1016/j.combustflame.2015.10.032.

References

[1] M. Altarawneh, B.Z. Dlugogorski, A mechanistic and kinetic study on the decomposition of morpholine, J. Phys. Chem. A 116 (29) (2012) 7703–7711.
[2] M.S. Rayson, M. Altarawneh, J.C. Mackie, E.M. Kennedy, B.Z. Dlugogorski, Theoretical study of the ammonia–hypochlorous acid reaction mechanism, J. Phys. Chem. A 114 (7) (2010) 2597–2606.
[3] A. Dean, J. Bozzelli, Combustion chemistry of nitrogen, in: W.C. Gardiner Jr. (Ed.), Gas-Phase Combustion Chemistry, Springer, New York, 2000, pp. 125–341.
[4] A. Williams, J.M. Jones, L. Ma, M. Pourkashanian, Pollutants from the combustion of solid biomass fuels, Prog. Energy Combust. Sci. 38 (2) (2012) 113–137.
[5] A. Lucassen, K. Zhang, J. Warkentin, K. Moshammer, P. Glarborg, P. Marshall, K. Kohse-Höinghaus, Fuel-nitrogen conversion in the combustion of small amines using dimethylamine and ethylamine as biomass-related model fuels, Combust. Flame 159 (7) (2012) 2254–2279.
[6] S. Li, D.F. Davidson, R.K. Hanson, Shock tube study of ethylamine pyrolysis and oxidation, Combust. Flame 161 (10) (2014) 2512–2518.
[7] S. Li, D.F. Davidson, R.K. Hanson, K. Moshammer, K. Kohse-Höinghaus, Shock tube study of ethylamine pyrolysis and oxidation, Proceedings of the 8th U.S. National Combustion Meeting, University of Utah, 2013, p. 19-22.
[8] M.H. Almatarneh, M. Altarawneh, R.A. Poirier, I.A. Saraireh, High level ab initio, DFT, and RRKM calculations for the unimolecular decomposition reaction of ethylamine, J. Comput. Sci. 5 (4) (2014) 568–575.
[9] A. Lucassen, N. Labbe, P.R. Westmoreland, K. Kohse-Höinghaus, Combustion chemistry and fuel-nitrogen conversion in a laminar premixed flame of morpholine as a model biofuel, Combust. Flame 158 (9) (2011) 1647–1666.
[10] M.J.E.A. Frisch, Gaussian 09, Wallingford CT, Gaussian, Inc, 2009.
[11] J.A. Montgomery, J.W. Ochterski, G.A. Petersson, A complete basis set model chemistry. IV. An improved atomic pair natural orbital method, J. Chem. Phys. 101 (7) (1994) 5900–5909.
[12] S. Canneaux, F. Bohr, E. Henon, KiSThelP, A Program to predict thermodynamic properties and rate constants from quantum chemistry results, J. Comput. Chem. 35 (1) (2014) 82–93.
[13] C. Eckart, The penetration of a potential barrier by electrons, Phys. Rev. 35 (1930) 1303–1309.
[14] Y. Zhao, N.E. Schultz, D.G. Truhlar, Design of density functionals by combining the method of constraint satisfaction with parametrization for thermochemistry, thermochemical kinetics, and noncovalent interactions, J. Chem. Theor. Comput. 2 (2) (2006) 364–382.
[15] R.K. Robinson, R.P. Lindstedt, A comparative ab initio study of hydrogen abstraction from *n*-propyl benzene, Combust. Flame 160 (12) (2013) 2642–2653.
[16] L. Sandhiya, K. Senthilkumar, Theoretical studies on mechanisms and kinetics of atsmospheric reactions, in: T. Ch, K. Han (Eds.), Reaction Rate Constant Computations: Theories and Applications, The Royal Society of Chemistry London, 2014, pp. 462–493.
[17] L. Masgrau, À. González-Lafont, J.M. Lluch, Variational transition-state theory rate constant calculations with multidimensional tunneling corrections of the reaction of acetone with OH., J. Phys. Chem. A 106 (48) (2002) 11760–11770.
[18] A. Fernández-Ramos, B. Ellingson, R. Meana-Pañeda, J.C. Marques, D. Truhlar, Symmetry numbers and chemical reaction rates, Theor. Chem. Account. 118 (4) (2007) 813–826.
[19] R.B. McClurg, R.C. Flagan, W.A. Goddard III, The hindered rotor density-of-states interpolation function, J. Chem. Phys. 106 (16) (1997) 6675–6680.
[20] J.R. Durig, Y.S. Li, Raman spectra of gases. XVIII. Internal rotational motions in ethylamine and ethylamine-D2, J. Chem. Phys. 63 (10) (1975) 4110–4113.
[21] F.L. Hirshfeld, Bonded-atom fragments for describing molecular charge densities, Theoret. Chim. Acta 44 (1977) 129–138.
[22] C. Fonseca Guerra, J.-W. Handgraaf, E.J. Baerends, F.M. Bickelhaupt, Voronoi deformation density (VDD) charges: assessment of the Mulliken, Bader, Hirshfeld, Weinhold, and VDD methods for charge analysis, J. Comput. Chem. 25 (2) (2004) 189–210.
[23] G. te Velde, F.M. Bickelhaupt, E.J. Baerends, C. Fonseca Guerra, S.J.A. van Gisbergen, J.G. Snijders, T Ziegler, Chemistry with ADF., J. Comput. Chem. 22 (9) (2001) 931–967.
[24] R.Y. Luo, Handbook of bond dissociation energies in organic compounds, CRC Press, Florida, Boca Raton, 1999.
[25] L. Onel, M. Blitz, M. Dryden, L. Thonger, P. Seakins, Branching ratios in reactions of oh radicals with methylamine, dimethylamine, and ethylamine, Environ. Sci. Technol. 48 (16) (2014) 9935–9942.
[26] R.K. Brinton, The abstraction of hydrogen atoms from amines and related compounds, Can. J. Chem. 38 (8) (1960) 1339–1345.
[27] P. Gray, A. Jones, Methyl radical reactions with ethylamine and deuterated ethylamines, Trans. Faraday Soc. 62 (0) (1966) 112–119.
[28] R.M. Marshall, H. Purnell, A. Sheppard, Reaction of hydrogen atoms with propane in the temperature range 298–534 K., J. Chem. Soc. Faraday Trans. 1 80 (11) (1984) 2999–3009.
[29] W. Tsang, Chemical kinetic data base for combustion chemistry. Part 3: propane, J. Phys. Chem. Ref. Data 17 (2) (1988) 887–951.
[30] Y. Hidaka, T. Oki, H. Kawano, Thermal decomposition of propane in shock waves, Int. J. Chem. Kinet. 21 (1989) 689–701.
[31] N. Ahubelem, M. Altarawneh, B.Z. Dlugogorski, Dehydrohalogenation of ethyl halides, Tetrahedron Lett. 55 (35) (2014) 4860–4868.
[32] M.M. Lynam, M. Kuty, J. Damborsky, J. Koca, P. Adriaens, Molecular orbital calculations to describe microbial reductive dechlorination of polychlorinated dioxins, Environ. Toxicol. Chem. 17 (6) (1998) 988–997.
[33] M. Wheeler, R. Mills, J.M. Roscoe, Temperature dependence of the rate coefficients for the reactions of Br atoms with dimethyl ether and diethyl ether, J. Phys. Chem. A 112 (5) (2008) 858–865.
[34] H.-H. Carstensen, A.M. Dean, O. Deutschmann, Rate constants for the H abstraction from alkanes (R–H) by radicals: A systematic study on the impact of R and R', Proc. Combust. Inst. 31 (1) (2007) 149–157.